

# Theory of a competitive spin liquid state for weak Mott insulators on the triangular lattice

Ryan V. Mishmash,<sup>1</sup> James R. Garrison,<sup>1</sup> Samuel Bieri,<sup>2</sup> and Cenke Xu<sup>1</sup>

<sup>1</sup>*Department of Physics, University of California, Santa Barbara, California 93106, USA*

<sup>2</sup>*Department of Physics, Massachusetts Institute of Technology, Cambridge, Massachusetts 02139, USA*

(Dated: July 22, 2013)

We propose a novel quantum spin liquid state that can explain many of the intriguing experimental properties of the low-temperature phase of the organic spin liquid candidate materials  $\kappa$ -(BEDT-TTF)<sub>2</sub>Cu<sub>2</sub>(CN)<sub>3</sub> and EtMe<sub>3</sub>Sb[Pd(dmit)<sub>2</sub>]<sub>2</sub>. This state of paired fermionic spinons preserves all symmetries of the system, and it has a gapless excitation spectrum with quadratic bands that touch at momentum  $\vec{k} = 0$ . This quadratic band touching is protected by symmetries. Using variational Monte Carlo techniques, we show that this state has highly competitive energy in the triangular lattice Heisenberg model supplemented with a realistically large ring-exchange term.

PACS numbers: 71.27.+a, 75.10.Jm, 75.10.Kt, 75.30.Kz

Quantum spin liquids are exotic phases of quantum spin systems which break no global symmetries even when thermal fluctuations are completely suppressed at zero temperature [1, 2]. In the last decade, candidates of gapless spin liquid phases have been discovered in various experimental systems, including  $\kappa$ -(BEDT-TTF)<sub>2</sub>Cu<sub>2</sub>(CN)<sub>3</sub> [3–5], EtMe<sub>3</sub>Sb[Pd(dmit)<sub>2</sub>]<sub>2</sub> [6–8], Ba<sub>3</sub>CuSb<sub>2</sub>O<sub>9</sub> [9], Ba<sub>3</sub>NiSb<sub>2</sub>O<sub>9</sub> [10], and ZnCu<sub>3</sub>(OH)<sub>6</sub>Cl<sub>2</sub> [11–13]. In all these materials, no evidence of magnetic order was found at temperatures much lower than the spin interaction energy scale of the system. In the current work, we will focus on the organic spin liquid materials  $\kappa$ -(BEDT-TTF)<sub>2</sub>Cu<sub>2</sub>(CN)<sub>3</sub> ( $\kappa$ -BEDT) and EtMe<sub>3</sub>Sb[Pd(dmit)<sub>2</sub>]<sub>2</sub> (DMIT). These materials are quasi-two-dimensional Mott insulators which are close to a Mott metal-insulator transition [5], and thus exhibit substantial local charge fluctuations. An effective spin model that may well describe the magnetic properties of these “weak” Mott insulators involves supplementing the usual (possibly extended) Heisenberg model with a four-site ring-exchange term [14, 15]. Here, we consider the following Hamiltonian:

$$H = J_1 \sum_{\langle i,j \rangle} 2\vec{S}_i \cdot \vec{S}_j + J_2 \sum_{\langle\langle i,j \rangle\rangle} 2\vec{S}_i \cdot \vec{S}_j + K \sum_{\langle i,j,k,l \rangle} (P_{ijkl} + \text{H.c.}), \quad (1)$$

where the sums  $\langle i,j \rangle$  and  $\langle\langle i,j \rangle\rangle$  go over all first- and second-neighbor links of the triangular lattice, respectively, while  $\langle i,j,k,l \rangle$  goes over all elementary four-site rhombi;  $P_{ijkl}$  rotates the spin configurations around a given rhombus. In what follows, we set  $J_1 = 1$  as the unit of energy.

The two different organic spin liquids  $\kappa$ -BEDT and DMIT share two universal properties:

1. At low temperatures, despite the fact that the system is still a Mott insulator for charge transport, the specific heat scales linearly with temperature:  $C_v = \gamma T$ . Furthermore,  $\gamma$  is essentially independent of a moderate

external magnetic field [3].

2. The spin susceptibility shows no magnetic phase transition at any finite temperature, and it saturates to a finite constant  $\chi$  at zero temperature [4].

These two phenomena are completely inconsistent with any semiclassical magnetic state and are strongly suggestive of the existence of a highly nontrivial quantum disordered phase. They also demonstrate the presence of a large density of charge-neutral excitations at low temperature. To date, four main theoretical scenarios have been proposed to describe these experimental facts:

1. In the U(1) spinon Fermi surface state [14, 16], a fermionic spinon  $f_{j\alpha}$  is introduced by decomposing the physical spin operator as  $\vec{S}_j = \frac{1}{2} \sum_{\alpha,\beta=\uparrow,\downarrow} f_{j\alpha}^\dagger \vec{\sigma}_{\alpha\beta} f_{j\beta}$  and taking the spinons to fill an ordinary Fermi sea at the mean-field level. This gives rise to a finite density of states, consistent with the experimental results mentioned above. Furthermore, it has been demonstrated that for strong enough ring exchange  $K$ , the spinon Fermi sea state has very competitive variational energy in the microscopic spin model (1) [14]. However, once we go beyond the mean-field level, the U(1) gauge fluctuation will acquire singular overdamped dynamics  $|\omega| \sim k^3$  due to its coupling with the Fermi surface [17]. This singular dynamics generates an even larger density of states at low temperature, which leads to a singular specific heat  $C_v \sim T^{2/3}$ . This specific heat behavior is not observed experimentally.

2. The most natural way to suppress the U(1) gauge fluctuation is to condense Cooper pairs of spinons and thus break the U(1) gauge fluctuation down to a fully gapped  $Z_2$  gauge fluctuation. This possibility has been explored numerically in Ref. [18], where the authors concluded that the particular pairing pattern that is energetically favored by Eq. (1) has nodal  $d_{x^2-y^2}$ -wave structure. However, this nodal  $d$ -wave pairing not only suppresses the gauge fluctuation, it also significantly suppresses the fermion density of states, and the system will no longer

have finite  $\gamma$  and  $\chi$  at low temperature, unless sufficient disorder is turned on.

3. Another very different approach was taken in Ref. [19], where the authors proposed that  $\kappa$ -BEDT is a  $Z_2$  spin liquid which is very close to the condensation quantum critical point of bosonic spinons. This quantum critical behavior is consistent with the NMR relaxation rate observed experimentally [20]. In particular, the small energy gap seen in thermal conductivity data [21] was identified with the gap of the topological defect of the  $Z_2$  spin liquid [19]. However, no parent spin Hamiltonian has been found for this state so far. Thus, it is unknown whether this quantum critical spin liquid can be realized in any experimentally relevant lattice model.

4. A novel Majorana slave fermion formalism was introduced in Ref. [22], where the authors proposed that the ground state of the organic spin liquids has a Majorana Fermi surface. But, just like the previous theory, so far it is unclear in which lattice model this spin liquid can be realized.

In this paper, we propose an entirely new spin liquid. In Ref. [23], possible  $Z_2$  spin liquids with an extended spinon Fermi surface were summarized. However, the spin liquid state proposed in the present paper is beyond the ones discussed in Ref. [23]. Our novel state has no spinon Fermi surface, but has a quadratic band touching (QBT) of fermionic spinons that is protected by the symmetry of the model:  $\omega \sim \pm k^2$ . In two dimensions, a quadratic band touching leads to a finite constant density of states, which automatically gives finite  $\gamma$  and  $\chi$  at zero temperature. Besides being consistent with the major experimental facts of the organic spin liquid compounds, this state has the following advantages:

1. As we will show below, this state is a very competitive variational ground state for model (1) in the physically relevant regime  $0.1 \lesssim K \lesssim 0.15$  and  $J_2 \simeq 0$  (see Fig. 1).

2. The gauge fluctuation for this state is fully gapped, and hence plays no role at low energy. Most field-theoretic calculations based on this state are thus well approximated at the mean-field level, and so, in contrast to the spinon Fermi surface state [24], they are well controlled.

3. Finite  $\gamma$  and  $\chi$  are *generic* properties of our QBT spin liquid. In contrast to the spinon Fermi surface state, these properties are both robust in the presence of gauge fluctuations, and unlike the nodal  $d$ -wave state, they do not rely on disorder.

4. A very small energy gap, much smaller than the Heisenberg exchange  $J_1$ , was observed by thermal conductivity measurements in  $\kappa$ -BEDT [21]. This small gap can be very elegantly explained by our QBT spin liquid without fine-tuning: an allowed short-range spinon interaction on top of our mean-field state may be marginally relevant, and thus naturally open up an exponentially small gap.

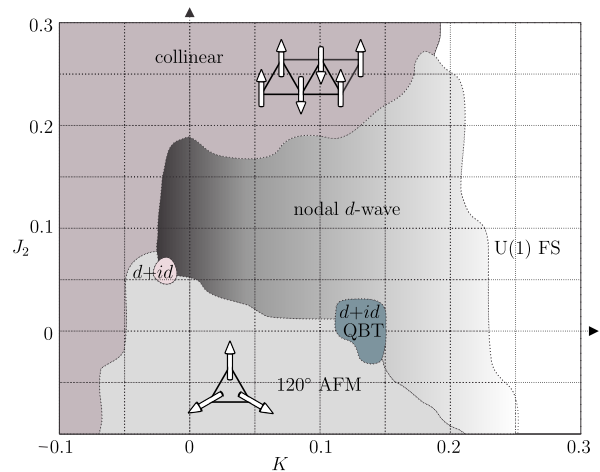


FIG. 1: Variational phase diagram of the spin Hamiltonian, Eq. (1). We propose that the  $d + id$  QBT spin liquid phase is a very strong candidate for the ground state of  $\kappa$ -BEDT and DMIT in the parameter range  $J_2 \simeq 0$  and  $K \simeq 0.13$ .

5. Since the gauge field fluctuation is fully gapped in our spin liquid, it does not respond to an external magnetic field. Thus our state has no obvious thermal Hall effect, which is consistent with experiments [25].

Let us first describe the QBT spin liquid state. We take the standard slave fermion (spinon) representation of spin-1/2 operators:  $\vec{S}_j = \frac{1}{2} \sum_{\alpha, \beta = \uparrow, \downarrow} f_{j\alpha}^\dagger \vec{\sigma}_{\alpha\beta} f_{j\beta}$ . The physical spin-1/2 Hilbert space is then recovered by imposing the on-site constraint  $\sum_{\alpha} f_{j\alpha}^\dagger f_{j\alpha} = 1$ , which introduces an  $SU(2)$  gauge symmetry to the low-energy dynamics of the spinons [26]. However, this  $SU(2)$  gauge symmetry will generally be broken by the mean-field dynamics, which can be described by a quadratic Hamiltonian of the form

$$H_{\text{MF}} = - \sum_{i,j} \left[ t_{ij} f_{i\sigma}^\dagger f_{j\sigma} + \left( \Delta_{ij} f_{i\uparrow}^\dagger f_{j\downarrow}^\dagger + \text{H.c.} \right) \right]. \quad (2)$$

The QBT spin liquid at the focus of this paper corresponds to a mean-field ansatz for the spinons with  $d + id$  pairing and vanishing hopping:

$$t_{ij} = 0, \quad \Delta_{j,j+\hat{e}} = \Delta(e_x + ie_y)^2. \quad (3)$$

Here,  $\hat{e}$  is a first-neighbor unit vector of the triangular lattice. This mean-field ansatz breaks the  $SU(2)$  gauge symmetry down to  $Z_2$ :  $f_\alpha \mapsto -f_\alpha$ . Thus, gauge fluctuations can be ignored in the low-energy dynamics of the system.

It is convenient to introduce a complex spinor  $\psi$  defined as  $(\psi_1, \psi_2) = (f_\uparrow, f_\downarrow)$ . Expanded at the  $\Gamma$ -point  $\vec{k} = 0$ , the low-energy Hamiltonian for the mean-field ansatz mentioned above reads

$$H_0 = \psi^\dagger \{ -\tau^x (\partial_x^2 - \partial_y^2) + 2\tau^y \partial_x \partial_y \} \psi. \quad (4)$$

This mean-field Hamiltonian has a quadratic band touching at  $\vec{k} = 0$ , which leads to a finite density of states in

two dimensions. We propose that this finite density of states is responsible for finite  $\gamma$  and  $\chi$  observed experimentally in  $\kappa$ -BEDT and DMIT. A similar QBT spin liquid state for the spin-1 material  $\text{Ba}_3\text{NiSb}_2\text{O}_9$  [10] was proposed in Ref. [27].

In addition to the quadratic band touching at  $\vec{k} = 0$ , there are also Dirac fermions at the corners of the Brillouin zone:  $\vec{Q}_{A,B} = \pm(4\pi/3, 0)$ . Complex Dirac fermion fields  $\psi_{A,B}$  at momenta  $\vec{Q}_{A,B}$  can be defined as  $\psi = \psi_A \exp(i\vec{Q}_A \cdot \vec{r}) + \psi_B \exp(i\vec{Q}_B \cdot \vec{r})$ . The low-energy Hamiltonian for  $\psi_{A,B}$  reads

$$H_{\pm(4\pi/3,0)} = \sum_{a=A,B} \psi_a^\dagger (-i\tau^x \partial_x - i\tau^y \partial_y) \psi_a. \quad (5)$$

At low temperature, the contribution of these Dirac fermions to  $\gamma$  and  $\chi$  is much smaller than the one resulting from the quadratic band touching at the  $\Gamma$ -point.

The spinon carries a projective representation of the physical symmetry group. In the Supplemental Material, we demonstrate that the mean-field QBT ansatz discussed above preserves all the symmetries of the model (including the spin symmetry, triangular lattice symmetry and time-reversal symmetry). As long as these symmetries are preserved, no relevant fermion bilinear terms can be added to Eqs. (4) and (5), and the low-energy dynamics is stable.

Let us now go beyond the mean field. As mentioned above, the mean-field ansatz breaks the gauge symmetry down to  $Z_2$ , and the gauge fluctuations are thus quite harmless. But, besides the gauge fluctuation, local short-range four-fermion interactions exist at both the Dirac points  $\vec{Q}_{A,B}$  and the QBT  $\Gamma$ -point. At the  $\Gamma$ -point, only the following four-fermion interaction needs to be considered:

$$H_4 = -g f_\uparrow^\dagger f_\uparrow f_\downarrow^\dagger f_\downarrow \sim g \psi_1^\dagger \psi_1 \psi_2^\dagger \psi_2. \quad (6)$$

The RG flow of this term is very simple: depending on the sign of  $g$ ,  $H_4$  can be either marginally relevant or irrelevant [28]. When it is relevant ( $g > 0$ ), the system spontaneously breaks time-reversal symmetry (it becomes a chiral spin liquid) and opens up an exponentially small gap at the  $\Gamma$ -point:  $m f_\alpha^\dagger f_\alpha = m \psi^\dagger \tau^z \psi$ . We identify this fluctuation generated gap with the small gap observed by thermal conductivity in  $\kappa$ -BEDT [21].

In DMIT, on the other hand, thermal conductivity measurements indicate that the system is gapless at the lowest temperature [25]. Thus, we conjecture that DMIT corresponds to the case with a marginally irrelevant  $H_4$  ( $g < 0$ ), while  $\kappa$ -BEDT corresponds to  $g > 0$ . The thermal conductivity behavior with negative  $g$  will be studied in detail in the future [29], taking into account both interaction and disorder effects.

Inspired by previous works [14, 18, 30–32], we now revisit the variational phase diagram of model (1) using a wide range of correlated spin wave functions. The

quadratic Hamiltonian, Eq. (2), allows straightforward construction of spin liquid wave functions by Gutzwiller projecting its ground state  $|\Psi_0\rangle$ . That is, we use as variational states  $|\Psi(\{t_{ij}\}, \{\Delta_{ij}\})\rangle = \mathcal{P}_G \mathcal{P}_N |\Psi_0\rangle$ , where  $\mathcal{P}_N$  is a projector to a state with  $N$  spinons, and  $N$  is the number of lattice sites ( $N_\uparrow = N_\downarrow = N/2$ ).  $\mathcal{P}_G = \prod_j [1 - n_{j\downarrow} n_{j\uparrow}]$  is the Gutzwiller projector which removes unphysical states containing doubly-occupied sites. We fix the spinon chemical potential  $\mu = t_{jj}$  such that  $|\Psi_0\rangle$  is half filled on average before projection, but other parameters in (2) are used as variational parameters. The evaluation of expectation values in such fermionic wave functions can be done efficiently and with high accuracy using variational Monte Carlo techniques [32–34]. For competing long-range ordered states, we use Jastrow-type wave functions as pioneered by Huse and Elser [35] (see the Supplemental Material for more details on all states we studied).

We first consider the case with  $J_2 = 0$  in Eq. (1). Since the seminal work of Motrunich [14] it has been known that the  $U(1)$  projected Fermi sea state (or “spin Bose metal” [30]) with isotropic nearest-neighbor  $t_{ij} = t$  and  $\Delta_{ij} = 0$  has remarkably good variational energy and is clearly the best fermionic trial state for relatively large ring exchange  $K \gtrsim 0.3$ . This state is also consistent with recent large-scale DMRG calculations on the four-leg ladder [31]. On the other hand, exact diagonalization studies [36] indicate that the  $120^\circ$  antiferromagnetic (AFM) order, which is believed to characterize the ground state of the Heisenberg model at  $K = 0$  [35, 37, 38], is destroyed at much smaller ring exchange  $K \gtrsim 0.1$ . Therefore, an intermediate spin liquid phase in the parameter regime  $0.1 \lesssim K \lesssim 0.3$  may well be present in the model, and is likely to be relevant for the organic compounds.

The most natural candidate states are  $Z_2$  spin liquids with finite spinon pairing  $\Delta_{ij} \neq 0$  in (2). Indeed, it has been known since the work of Motrunich that in the intermediate parameter regime of Eq. (1) such projected Bardeen-Cooper-Schrieffer states do have significantly lower energy than the  $120^\circ$  AFM and  $U(1)$  Fermi sea states. However, the nature of the spinon pairing pattern in this putative  $Z_2$  spin liquid was still up for debate. In this paper, we perform accurate large-scale simulations up to  $30 \times 30$  lattice sites to check all singlet ( $\Delta_{ij} = \Delta_{ji}$ ) and triplet ( $\Delta_{ij} = -\Delta_{ji}$ ) pairing instabilities ( $s$ ,  $p$ ,  $p + ip$ ,  $d$ ,  $d + id$ , and  $f$ -wave) of the  $U(1)$  Fermi sea state in model (1). We find the remarkable result that for  $0.1 \lesssim K \lesssim 0.15$  our QBT  $d + id$  state, as discussed above, is highly competitive, and perhaps has the lowest energy of *any* projected fermionic trial state, including the nodal  $d$ -wave state of Ref. [18].

The results of our variational study at  $J_2 = 0$  are summarized in Fig. 2. Consistent with Refs. [14, 18], we find that the unpaired  $U(1)$  Fermi sea (FS) state and states with nodal  $d$ -wave and  $d + id$  pairing symmetries are the most competitive spin liquid wave functions for

this model. The gap functions for the  $d + id$  and nodal  $d$ -wave states are given by  $\Delta_{j,j+\hat{e}}^{(d+id)} = \Delta(e_x + ie_y)^2$  and  $\Delta_{j,j+\hat{e}}^{(\text{nodal } d)} = \Delta(e_x^2 - e_y^2)$ , respectively, where  $\hat{e}$  is a unit vector connecting nearest neighbors on the triangular lattice. Each of these ansätze thus has one variational parameter  $\Delta/t$  which we parameterize by  $\alpha = \tan^{-1}(\Delta/t)$ . In the top panel of Fig. 2, we show the optimal energies per site,  $E_{\text{minimum}}$ , versus ring exchange  $K$  for the  $d + id$ , nodal  $d$ -wave, U(1) FS, and  $120^\circ$  AFM states. In the bottom panel, we show the corresponding optimal  $\alpha$  for both the  $d + id$  and nodal  $d$ -wave states. We see that the  $120^\circ$  AFM state wins for  $K \lesssim 0.1$ ; however, immediately upon exiting the  $120^\circ$  phase for  $0.1 \lesssim K \lesssim 0.15$ , the  $d + id$  and nodal  $d$ -wave states are extremely close in energy and are basically degenerate within statistical error. Remarkably, as seen in the bottom panel of Fig. 2, the optimal  $d + id$  state in the entire range  $0.1 \lesssim K \lesssim 0.17$  is in fact our exotic QBT state of interest, that is  $\Delta/t \rightarrow \infty, \alpha = \pi/2$ . For still larger  $K$ ,  $0.15 \lesssim K \lesssim 0.25$ , the optimal ansatz is the nodal  $d$ -wave state, a result which is consistent with Ref. [18]. Finally, for  $K \gtrsim 0.25$ , the optimal pairing am-

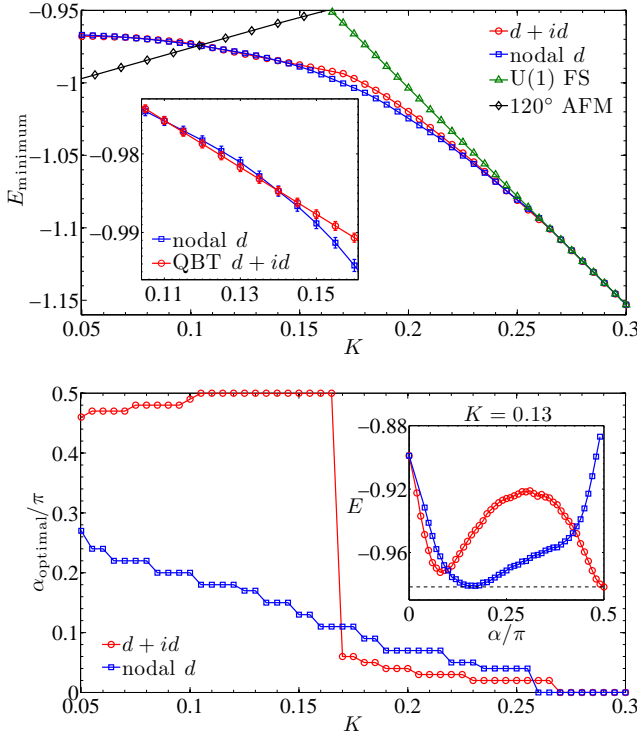


FIG. 2: Upper panel: Variational energies per site for the Hamiltonian, Eq. (1), at  $J_2 = 0$  as a function of  $K$  for the most competitive trial states in our study; in the inset, we show a zoom of the region of the phase diagram where the QBT  $d + id$  state is most competitive. Lower panel: The optimal variational parameter  $\alpha = \tan^{-1}(\Delta/t)$  is plotted for the  $d + id$  and nodal  $d$ -wave states; in the inset, we show the variational energies for all  $\alpha$  at the point  $K = 0.13$  where the dashed line indicates the energy of the QBT state.

plitude  $\Delta \rightarrow 0$  for all spin liquid states, thus describing a crossover to the U(1) Fermi sea state of Refs. [14, 30, 31].

In the inset of the bottom panel of Fig. 2, we plot the variational energies per site versus  $\alpha$  at the point  $K = 0.13$  in the spin liquid phase. Interestingly, there are two local minima for the  $d + id$  ansatz: the first minimum at small  $\Delta \lesssim t$  is smoothly connected to the U(1) Fermi sea state at  $\Delta = 0$ , while the second minimum at  $\Delta/t \rightarrow \infty$  is the qualitatively new QBT state at the focus of our work. For  $0.1 \lesssim K \lesssim 0.17$ , the latter is lower in energy than the former, but is almost degenerate with the optimal nodal  $d$ -wave state which always has small  $\Delta \lesssim t$ . Indeed, the two local minima in the  $d + id$  ansatz are already present in the pure Heisenberg model ( $K = J_2 = 0$ ), with a large- $\Delta$  state ( $\alpha = 0.44, \Delta/t = 5.2$ ) having minimum energy. Furthermore, the QBT state at  $\alpha = \pi/2$  has surprisingly low ring-term expectation value, and this conspires with the good Heisenberg energy of the generic large- $\Delta$   $d + id$  state to make the QBT state the optimal fermionic spin liquid ansatz in the parameter window  $0.1 \lesssim K \lesssim 0.15$ . (For more details, see the Supplemental Material.)

The authors of Ref. [18] concluded that the nodal  $d$ -wave state is clearly the best variational ground state for intermediate  $0.1 \lesssim K \lesssim 0.15$ . We believe that there are two reasons for this discrepancy with our result. First, Ref. [18] considered only a restricted range of small  $\Delta/t$  for the  $d + id$  ansatz which excluded the QBT state altogether. Second, our extensive finite-size analysis shows that quite large lattice clusters ( $\gtrsim 18 \times 18$  sites) are necessary to get well converged expectation values for the nodal  $d$ -wave state. Our calculations find poorly converged expectation values and strong dependencies on the spinon boundary conditions for a nodal  $d$ -wave state on the small  $10 \times 11$  cluster that was used in [18].

Finally, we discuss the effect of a second-neighbor interaction  $J_2$ . In Fig. 1, we present a variational phase diagram in the  $K$ - $J_2$  plane. A ferromagnetic interaction ( $J_2 < 0$ ) quickly favors the  $120^\circ$  AFM state over the QBT  $d + id$  state and destroys the spin liquid phase. On the other hand, antiferromagnetic  $J_2 > 0$  strongly frustrates the  $120^\circ$  AFM state and favors a nodal  $d$ -wave spin liquid. Negative ring-exchange or larger values of  $J_2 \gtrsim 0.17$  lead to a collinear phase. In Fig. 1, around  $J_2 \simeq 0.05$  and  $K \simeq -0.02$ , a small fully gapped  $d + id$  phase with finite  $\Delta/t$  emerges. This is a chiral spin liquid with non-trivial topological order [39, 40]. Our preliminary results show that this phase will expand significantly once an antiferromagnetic third-neighbor Heisenberg coupling  $J_3$  is added to Eq. (1). More details on this phase will be elaborated in future work.

The ability of the nodal  $d$ -wave state to beat the collinear state for  $K \simeq 0$  may suggest (see Refs. [41, 42]) that we are overestimating the extent of the nodal  $d$ -wave state in our phase diagram (see also the Supplemental Material). Of course, a variational study can never claim to have the final say on the phase diagram of a given



microscopic model, and quantitative locations of phase boundaries should not be taken too seriously. What is very robust, however, is the statement that our QBT  $d+id$  state has both extremely competitive energetics in a realistic parameter regime and highly appealing phenomenology for the organic spin liquid compounds.

The authors would like to thank T. Grover, P. A. Lee, T. Senthil, B. K. Clark, and M. P. A. Fisher for helpful discussions. We are especially grateful to O. I. Motrunich for enlightening discussions and for sharing of his early variational Monte Carlo data. We also thank Fa Wang for discussions at the beginning of this project. R.V.M. and J.R.G. are supported by NSF grant DMR-1101912. S.B. is supported by NSF grant DMR-1104498. C.X. is supported by NSF grant DMR-1151208 and the Packard Fellowship. This work was made possible by the computing facilities of the Center for Scientific Computing from CNSI, MRL (NSF MRSEC award DMR-1121053), and NSF grant CNS-0960316; and by the computing cluster of the MIT Physics Department.

- 
- [1] L. Balents, *Nature* **464**, 199 (2010).
  - [2] P. A. Lee, *Science* **321**, 1306 (2008).
  - [3] S. Yamashita *et al.*, *Nature Physics* **4**, 459 (2008).
  - [4] Y. Shimizu, K. Miyagawa, K. Kanoda, M. Maesato, and G. Saito, *Phys. Rev. Lett.* **91**, 107001 (2003).
  - [5] Y. Kurosaki, Y. Shimizu, K. Miyagawa, K. Kanoda, and G. Saito, *Phys. Rev. Lett.* **95**, 177001 (2005).
  - [6] T. Itou, A. Oyamada, S. Maegawa, M. Tamura, and R. Kato, *Journal of Physics: Conference Series* **145**, 012039 (2009).
  - [7] T. Itou, A. Oyamada, S. Maegawa, M. Tamura, and R. Kato, *Physical Review B* **77**, 104413 (2008).
  - [8] Y. Shimizu, H. Akimoto, H. Tsujii, A. Tajima, and R. Kato, *Journal of Physics: Condensed Matter* **19**, 145240 (2007).
  - [9] H. D. Zhou *et al.*, *Phys. Rev. Lett.* **106**, 147204 (2011).
  - [10] J. G. Cheng, G. Li, L. Balicas, J. S. Zhou, J. B. Goodenough, C. Xu, and H. D. Zhou, *Phys. Rev. Lett.* **107**, 197204 (2011).
  - [11] J. S. Helton *et al.*, *Phys. Rev. Lett.* **98**, 107204 (2007).
  - [12] J. S. Helton *et al.*, *Phys. Rev. Lett.* **104**, 147201 (2010).
  - [13] B. Fåk *et al.*, *Phys. Rev. Lett.* **109**, 037208 (2012).
  - [14] O. I. Motrunich, *Phys. Rev. B* **72**, 045105 (2005).
  - [15] G. Misguich, C. Lhuillier, B. Bernu, and C. Waldtmann, *Phys. Rev. B* **60**, 1064 (1999).
  - [16] S.-S. Lee and P. A. Lee, *Phys. Rev. Lett.* **95**, 036403 (2005).
  - [17] J. Polchinski, *Nucl. Phys. B* **422**, 617 (1994).
  - [18] T. Grover, N. Trivedi, T. Senthil, and P. A. Lee, *Phys. Rev. B* **81**, 245121 (2010).
  - [19] Y. Qi, C. Xu, and S. Sachdev, *Phys. Rev. Lett.* **102**, 176401 (2009).
  - [20] Y. Shimizu, K. Miyagawa, K. Kanoda, M. Maesato, and G. Saito, *Physical Review B* **73**, 140407(R) (2006).
  - [21] M. Yamashita *et al.*, *Nature Physics* **5**, 44 (2009).
  - [22] R. R. Biswas, L. Fu, C. R. Laumann, and S. Sachdev, *Phys. Rev. B* **83**, 245131 (2011).
  - [23] M. Barkeshli, H. Yao, and S. A. Kivelson, *Phys. Rev. B* **87**, 140402(R) (2013).
  - [24] S.-S. Lee, *Phys. Rev. B* **80**, 165102 (2009).
  - [25] M. Yamashita *et al.*, *Science* **328**, 1246 (2010).
  - [26] X.-G. Wen, *Phys. Rev. B* **65**, 165113 (2002).
  - [27] C. Xu, F. Wang, Y. Qi, L. Balents, and M. P. A. Fisher, *Phys. Rev. Lett.* **108**, 087204 (2012); Note that an extra color index of the slave fermion has to be introduced for spin-1 systems. See also Ref. [34].
  - [28] K. Sun, H. Yao, E. Fradkin, and S. A. Kivelson, *Phys. Rev. Lett.* **103**, 046811 (2009).
  - [29] Eun-Gook Moon and Cenke Xu, in progress (2013).
  - [30] D. N. Sheng, O. I. Motrunich, and M. P. A. Fisher, *Phys. Rev. B* **79**, 205112 (2009).
  - [31] M. S. Block, D. N. Sheng, O. I. Motrunich, and M. P. A. Fisher, *Phys. Rev. Lett.* **106**, 157202 (2011).
  - [32] C. Gros, *Phys. Rev. B* **38**, 931(R) (1988); *Ann. Phys. (N.Y.)* **189**, 53 (1989).
  - [33] D. Ceperley, G. V. Chester, and M. H. Kalos, *Phys. Rev. B* **16**, 3081 (1977).
  - [34] S. Bieri, M. Serbyn, T. Senthil, and P. A. Lee, *Phys. Rev. B* **86**, 224409 (2012).
  - [35] D. A. Huse and V. Elser, *Phys. Rev. Lett.* **60**, 2531 (1988).
  - [36] W. LiMing, G. Misguich, P. Sindzingre, and C. Lhuillier, *Phys. Rev. B* **62**, 6372 (2000).
  - [37] L. Capriotti, A. E. Trumper, and S. Sorella, *Phys. Rev. Lett.* **82**, 3899 (1999).
  - [38] S. R. White and A. L. Chernyshev, *Phys. Rev. Lett.* **99**, 127004 (2007).
  - [39] V. Kalmeyer and R. B. Laughlin, *Phys. Rev. Lett.* **59**, 2095 (1987).
  - [40] X.-G. Wen, F. Wilczek, and A. Zee, *Phys. Rev. B* **39**, 11413 (1989).
  - [41] T. Jolicoeur, E. Dagotto, E. Gagliano, and S. Bacci, *Phys. Rev. B* **42**, 4800 (1990).
  - [42] P. Lecheminant, B. Bernu, C. Lhuillier, and L. Pierre, *Phys. Rev. B* **52**, 6647 (1995).
  - [43] A. C. Potter and P. A. Lee, arXiv:1303.6956 (unpublished).
  - [44] G. Misguich, C. Lhuillier, B. Bernu, and C. Waldtmann, *Phys. Rev. B* **60**, 1064 (1999).
  - [45] T. Momoi, K. Kubo, and K. Niki, *Phys. Rev. Lett.* **79**, 2081 (1997).
  - [46] L. Messio, C. Lhuillier, and G. Misguich, *Phys. Rev. B* **83**, 184401 (2011).
  - [47] Interestingly, in contrast to the SU(2) case discussed in the present paper, Gutzwiller projected density wave states with three flavors of fermionic spinons clearly outperform Huse-Elser wave functions for SU(3) antiferromagnets on the triangular lattice [34].
  - [48] O. I. Motrunich, private communications.
  - [49] S.-S. Lee, P. A. Lee, and T. Senthil, *Phys. Rev. Lett.* **98**, 067006 (2007).

## Supplementary Materials

### A: Projective symmetry group analysis of the QBT $d + id$ $Z_2$ spin liquid

We take the standard slave fermion representation of the spin-1/2 operator at site  $j$ :

$$\hat{S}_j^\mu = \frac{1}{2} \sum_{\alpha, \beta = \uparrow, \downarrow} f_{j\alpha}^\dagger \sigma_{\alpha\beta}^\mu f_{j\beta}. \quad (7)$$

The gauge symmetry of this representation is  $SU(2)$ , denoted as  $SU(2)_g$ . In order to make both spin  $SU(2)$  symmetry  $[SU(2)_s]$  and gauge  $SU(2)$  symmetry manifest, it is convenient to define the following Majorana fermion  $\eta$ :

$$f_{j\alpha} = \frac{1}{2}(\eta_{j,\alpha,1} + i\eta_{j,\alpha,2}). \quad (8)$$

On every site,  $\eta_j$  has in total two two-component spaces, making the maximal possible transformation on  $\eta_j$   $SO(4)$ . Within this  $SO(4)$ , the  $SU(2)_s$  transformations and  $SU(2)_g$  transformations are generated by the following operators:

$$\begin{aligned} SU(2)_s &: (\sigma^x \lambda^y, \sigma^y, \sigma^z \lambda^y), \\ SU(2)_g &: (\sigma^y \lambda^z, \sigma^y \lambda^x, \lambda^y), \end{aligned} \quad (9)$$

where the Pauli matrices  $\lambda^a$  operate on the two-component space  $(\text{Re}[f], \text{Im}[f])$ .  $SU(2)_s$  and  $SU(2)_g$  commute with each other.

In terms of slave fermions  $f_\alpha$ , the Heisenberg model reads

$$\begin{aligned} \sum_{i,j,\mu} J_{ij} \hat{S}_i^\mu \hat{S}_j^\mu &\sim \sum_{i,j,\mu} J_{ij} f_{i\alpha}^\dagger \sigma_{\alpha\beta}^\mu f_{i\beta} f_{j\gamma}^\dagger \sigma_{\gamma\rho}^\mu f_{j\rho} \\ &\sim -2J_{ij} \hat{\Delta}_{ji}^* \hat{\Delta}_{ji} + \text{Const}, \\ \hat{\Delta}_{ji} &= \varepsilon_{\alpha\beta} f_{j\alpha} f_{i\beta}. \end{aligned} \quad (10)$$

The QBT  $d + id$  spin liquid state studied in this paper corresponds to the following mean-field ansatz:

$$\langle \hat{\Delta}_{j,j+\hat{e}} \rangle \equiv \Delta_{j,j+\hat{e}} = \Delta^{(m)}(e_x + ie_y)^2. \quad (11)$$

Here,  $\Delta^{(m)}$  denotes first- ( $m = 1$ ) and second-neighbor ( $m = 2$ ) pairing amplitudes, and  $\hat{e}$  are the corresponding unit vectors on the triangular lattice.

Expanded at  $\vec{k} = 0$ , the low-energy mean-field Hamiltonian reads

$$H_0 \sim \eta^\dagger \{ -\sigma^y \lambda^x (\partial_x^2 - \partial_y^2) + 2\sigma^y \lambda^z \partial_x \partial_y \} \eta. \quad (12)$$

This mean-field Hamiltonian has quadratic band-touching (QBT) at  $\vec{k} = 0$ , and the gauge symmetry is broken down to  $Z_2$ :  $\eta \mapsto -\eta$ .

For a finite range around  $\Delta^{(2)}/\Delta^{(1)} \simeq 0$ , in addition to the quadratic band touching at  $\vec{k} = 0$ , there

are also Dirac fermions at the Brillouin zone corners  $\vec{Q} = \pm(4\pi/3, 0)$ . A complex Dirac fermion field  $\chi$  at momentum  $\vec{Q} = (4\pi/3, 0)$  can be defined as

$$\eta_{\vec{r}} = \chi_{\vec{r}} e^{i\vec{Q} \cdot \vec{r}} + \chi_{\vec{r}}^\dagger e^{-i\vec{Q} \cdot \vec{r}}. \quad (13)$$

The low-energy Hamiltonian for  $\chi$  reads

$$H_\chi \sim \chi^\dagger (-i\sigma^y \lambda^x \partial_x - i\sigma^y \lambda^z \partial_y) \chi. \quad (14)$$

The spinon carries a projective representation of the physical symmetry group, and under discrete symmetry transformations, the low-energy fields  $\eta$  and  $\chi$  transform as

$$\begin{aligned} T_x &: x \mapsto x + 1, \quad \eta \mapsto \eta, \quad \chi \mapsto e^{i4\pi/3} \chi; \\ T &: t \mapsto -t, \quad \eta \mapsto i\lambda^y \eta, \quad \chi \mapsto i\lambda^y \chi^\dagger; \\ \mathcal{I} &: \vec{r} \mapsto -\vec{r}, \quad \eta \mapsto \eta, \quad \chi \mapsto \chi^\dagger; \\ P_y &: x \mapsto -x, \quad \eta \mapsto i\sigma^y \lambda^x \eta, \quad \chi \mapsto i\sigma^y \lambda^x \chi^\dagger; \\ R_{\pi/3} &: (x + iy) \mapsto e^{i\pi/3}(x + iy), \quad \eta \mapsto e^{i\frac{\pi}{3}\lambda^y} \eta, \\ &\quad \chi \mapsto e^{i\frac{\pi}{3}\lambda^y} \chi^\dagger. \end{aligned} \quad (15)$$

Importantly, notice that our QBT  $d + id$  state is invariant under all the discrete symmetries, including time reversal, reflection, rotation, etc.

With these symmetries, no fermion bilinears are allowed to be added to the low-energy mean-field Hamiltonian. For example, a fermion bilinear  $\eta^\dagger \lambda^y \eta \sim f^\dagger f$  at the  $\Gamma$ -point would gap out the QBT producing a chiral spin liquid, but it is not allowed by time-reversal symmetry. On the other hand, a marginally relevant four-fermion interaction can lead to *spontaneous* time-reversal symmetry breaking and generate an exponentially small gap  $m\eta^\dagger \lambda^y \eta$  (see also the main text).

Finally, we mention that on a finite sample, the QBT spin liquid exhibits a pair of dispersionless edge modes at the mean-field level. However, we expect that these edge modes will be unstable when weak interactions are taken into account [43].

### B: Details and discussion of our VMC calculations

For the variational Monte Carlo (VMC) results presented in this paper, we typically used  $\sim 10^6$  equilibrium sweeps, and averaged over 2000 spin configurations obtained from  $\sim 10^6$  measurement sweeps. In estimating the error of our measurements, we used a binning analysis with  $\sim 20$  samples per bin. In our plots, all errors are either on the order of or smaller than the symbol size, or explicitly depicted with one-sigma error bars.

To avoid degeneracies or singularities in the spin liquid wave functions, we work with a mean-field Hamiltonian,

Eq. (2) of the main text, with spinon boundary conditions periodic in one direction and antiperiodic in the other direction; this ensures a spin wave function with fully periodic boundary conditions. We have carefully checked that our measurements, e.g.,  $\langle \vec{S}_i \cdot \vec{S}_j \rangle$  and  $\langle P_{ijkl} + \text{H.c.} \rangle$ , are converged in the system size  $L_x \times L_y$  and do not depend on the spinon boundary conditions. The final energetics data presented in Fig. 2 of the main text, as well as in Figs. 3 and 4 below, was taken on a  $30 \times 30$  lattice.

For the ordered states, we use three-sublattice  $120^\circ$  antiferromagnetic (AFM) [14, 35] and four-sublattice [41] states that are suggested within a spin-wave analysis of the model at  $K = 0$ . Such ground state ordering patterns ( $120^\circ$  AFM and collinear) were also found in exact diagonalization calculations on small lattice clusters [36, 41, 42, 44]. Furthermore, we have checked the possibility of spiral orders with arbitrary wave vectors (commensurate with the system size). We have not considered the non-planar state proposed in [45, 46], leaving this for future work.

We note that quadratic fermion Hamiltonians similar to Eq. (2) of the main text can be used to construct states exhibiting magnetic order [32, 34]. However, it turns out that such Gutzwiller projected spin-density wave states do not give good variational energies. In our case of triangular-lattice spin-1/2 antiferromagnets, much better wave functions can be obtained by applying spin-Jastrow factors to product states, as pioneered in [35]. We use such Huse-Elser wave functions with first- and second-neighbor Jastrow factors to compare their energies with those of the spin liquid states, and to map out the variational phase diagram of the model [47].

The variational phase diagram we obtain for the parameter range and states considered is shown in Fig. 1 of the main text. On the line  $K = 0$ , we find that the  $120^\circ$  AFM state is stable up to  $J_2 \lesssim 0.05$ , at which point a nodal  $d$ -wave spin liquid starts to have the lowest energy within our set of wave functions. It should be noted

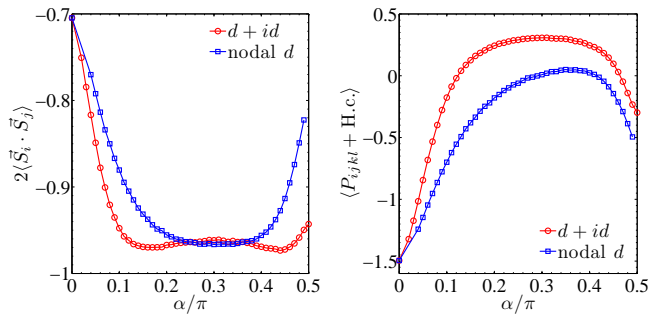


FIG. 3: First-neighbor Heisenberg exchange (left) and ring exchange (right) expectation values per site for the  $d+id$  and nodal  $d$ -wave states as a function of  $\alpha = \tan^{-1}(\Delta/t)$ . In the case of  $d+id$ , the special QBT point lies at  $\alpha/\pi = 0.5$ .

that on the line  $K = 0$ , spin-wave calculations predict a transition from the  $120^\circ$  AFM state to a collinear phase at  $J_2 = 0.125$  [41]. Exact diagonalization results seem to support a scenario without an intermediate spin liquid phase [42]. It is therefore possible that our variational approach overestimates the spin liquid regions with respect to the ordered states, especially in the case of the nodal  $d$ -wave spin liquid. Also, we have not considered spin liquids obtained by spinon hopping patterns with finite fluxes, as the ring term strongly disfavors such states [14] (although Motrunich [48] has found the time-reversal invariant “ $U1B$ ” state with alternating 0 and  $\pi$  fluxes through the triangles to be a promising ground state candidate for  $K \simeq 0$  and  $J_2 \gtrsim 0$ ). Interestingly, the zero-flux  $U(1)$  spin liquid at  $K \gtrsim 0.25$  is quite stable with respect to second-neighbor interaction  $J_2$ , and it is not destroyed within the parameter range and states we considered.

Finally, on the line  $J_2 = 0$ , Motrunich [14, 48] found a transition to a spin liquid phase at  $K \gtrsim 0.14$ . This small discrepancy with the transition point we find in the present paper may be traced back to the fact that we did not keep as many variational parameters in our Huse-Elser wave functions, and that he considered a more restricted set of spin liquid states. We leave a systematic study of the effect of more parameters in all our wave functions for future work. However, we expect that the spin liquid phase space may only slightly shrink, and that the basic conclusions of our study remain unchanged.

Let us briefly discuss other variational quantum spin liquid wave functions that we have also considered, but that were not mentioned in the main text. We have generalized  $s$ - and  $d$ -wave states by allowing three independent real singlet pairings  $\Delta_{ij}$  on first-neighbor links. Furthermore, we have checked the possibility of finite-momentum pairing instabilities of the  $U(1)$  spin liquid as proposed in [49] with the “Amperean pairing” state. However, we could not find convincing evidence that such states are realized in the model, Eq. (1) of the main text.

Finally, in order to further improve the energy of the

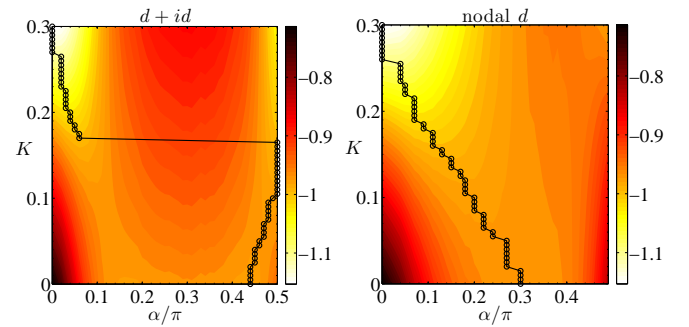


FIG. 4: Contour plots of the trial energy per site versus  $K$  and  $\alpha = \tan^{-1}(\Delta/t)$  for the  $d+id$  (left) and nodal  $d$ -wave (right) states ( $J_2 = 0$ ). The black curves indicate the optimal  $\alpha$  for each  $K$  (see also Fig. 2 of the main text, bottom panel).

QBT  $d + id$  state, we set the hopping  $t_{ij} = 0$  and added a second-neighbor pairing amplitude  $\Delta^{(2)}$  to the trial Hamiltonian, Eq. (2) of the main text. However, we found that the optimal parameter is always essentially  $\Delta^{(2)}/\Delta^{(1)} \simeq 0$  for the model considered.

### C: Details of the energy landscape for the $d + id$ and nodal $d$ -wave states

We can gain further intuition for the energetics (at  $J_2 = 0$ ) of the first-neighbor  $d + id$  and nodal  $d$ -wave states by considering the  $\alpha$ -dependence [ $\alpha = \tan^{-1}(\Delta/t)$ ] of expectation values  $2\langle \vec{S}_i \cdot \vec{S}_j \rangle$  and  $\langle P_{ijkl} + \text{H.c.} \rangle$  used to compute the variational energy per site:  $E = J_1 [2\langle \vec{S}_i \cdot \vec{S}_j \rangle] + K [\langle P_{ijkl} + \text{H.c.} \rangle]$ . These results are shown in Fig. 3. We find the striking result that the two local minima in the  $d + id$  ansatz discussed in the main text are actually present already in the pure Heisenberg model, with the *large- $\Delta$*  state ( $\alpha/\pi \simeq 0.44$ ,  $\Delta/t \simeq 5.2$ ) slightly lower in energy (see Fig. 3, left panel). Furthermore, we see in the right panel of Fig. 3 that beyond some large value of  $\Delta$  ( $\alpha/\pi \simeq 0.4$ ), we can gain substantial ring energy in both the  $d + id$  and nodal  $d$ -wave states by actually further increasing  $\Delta$ . In the case of  $d + id$ , going to the extreme limit  $\Delta/t \rightarrow \infty$  loses only somewhat marginal Heisenberg energy while at the same time gains significant ring energy: It is ultimately a balance between these two effects which makes the QBT  $d + id$  state highly competitive in the intermediate parameter regime of the ring model.

Finally, in Fig. 4 we show contour plots of the trial energy versus both  $K$  and  $\alpha$  (for which the inset of the bottom panel of Fig. 2 of the main text is a cross section). For the  $d + id$  state (left panel), we can clearly see two basins of local minima: one of which connects to the QBT state at  $\alpha = \pi/2$ , the other of which connects to the U(1) state at  $\alpha = 0$ . Upon increasing  $K$  out of the pure Heisenberg model, the large- $\Delta$   $d + id$  state quickly tracks to the QBT state near  $K \simeq 0.1$ , at which it remains until  $K \simeq 0.17$  where the optimal  $d + id$  state dramatically changes to one with small  $\Delta$ . These results clearly show that the QBT  $d + id$  state is a qualitatively new phase, and that it is not continuously connected to the U(1) Fermi sea state at  $\Delta = 0$ . In sharp contrast, the optimal nodal  $d$ -wave state (right panel) is continuously connected to the U(1) state for all values of  $K$ .

---

[1] L. Balents, Nature **464**, 199 (2010).  
[2] P. A. Lee, Science **321**, 1306 (2008).  
[3] S. Yamashita *et al.*, Nature Physics **4**, 459 (2008).  
[4] Y. Shimizu, K. Miyagawa, K. Kanoda, M. Maesato, and G. Saito, Phys. Rev. Lett. **91**, 107001 (2003).

[5] Y. Kurosaki, Y. Shimizu, K. Miyagawa, K. Kanoda, and G. Saito, Phys. Rev. Lett. **95**, 177001 (2005).  
[6] T. Itou, A. Oyamada, S. Maegawa, M. Tamura, and R. Kato, Journal of Physics: Conference Series **145**, 012039 (2009).  
[7] T. Itou, A. Oyamada, S. Maegawa, M. Tamura, and R. Kato, Physical Review B **77**, 104413 (2008).  
[8] Y. Shimizu, H. Akimoto, H. Tsujii, A. Tajima, and R. Kato, Journal of Physics: Condensed Matter **19**, 145240 (2007).  
[9] H. D. Zhou *et al.*, Phys. Rev. Lett. **106**, 147204 (2011).  
[10] J. G. Cheng, G. Li, L. Balicas, J. S. Zhou, J. B. Goodenough, C. Xu, and H. D. Zhou, Phys. Rev. Lett. **107**, 197204 (2011).  
[11] J. S. Helton *et al.*, Phys. Rev. Lett. **98**, 107204 (2007).  
[12] J. S. Helton *et al.*, Phys. Rev. Lett. **104**, 147201 (2010).  
[13] B. Fåk *et al.*, Phys. Rev. Lett. **109**, 037208 (2012).  
[14] O. I. Motrunich, Phys. Rev. B **72**, 045105 (2005).  
[15] G. Misguich, C. Lhuillier, B. Bernu, and C. Waldtmann, Phys. Rev. B **60**, 1064 (1999).  
[16] S.-S. Lee and P. A. Lee, Phys. Rev. Lett. **95**, 036403 (2005).  
[17] J. Polchinski, Nucl. Phys. B **422**, 617 (1994).  
[18] T. Grover, N. Trivedi, T. Senthil, and P. A. Lee, Phys. Rev. B **81**, 245121 (2010).  
[19] Y. Qi, C. Xu, and S. Sachdev, Phys. Rev. Lett. **102**, 176401 (2009).  
[20] Y. Shimizu, K. Miyagawa, K. Kanoda, M. Maesato, and G. Saito, Physical Review B **73**, 140407(R) (2006).  
[21] M. Yamashita *et al.*, Nature Physics **5**, 44 (2009).  
[22] R. R. Biswas, L. Fu, C. R. Laumann, and S. Sachdev, Phys. Rev. B **83**, 245131 (2011).  
[23] M. Barkeshli, H. Yao, and S. A. Kivelson, Phys. Rev. B **87**, 140402(R) (2013).  
[24] S.-S. Lee, Phys. Rev. B **80**, 165102 (2009).  
[25] M. Yamashita *et al.*, Science **328**, 1246 (2010).  
[26] X.-G. Wen, Phys. Rev. B **65**, 165113 (2002).  
[27] C. Xu, F. Wang, Y. Qi, L. Balents, and M. P. A. Fisher, Phys. Rev. Lett. **108**, 087204 (2012); Note that an extra color index of the slave fermion has to be introduced for spin-1 systems. See also Ref. [34].  
[28] K. Sun, H. Yao, E. Fradkin, and S. A. Kivelson, Phys. Rev. Lett. **103**, 046811 (2009).  
[29] Eun-Gook Moon and Cenke Xu, in progress (2013).  
[30] D. N. Sheng, O. I. Motrunich, and M. P. A. Fisher, Phys. Rev. B **79**, 205112 (2009).  
[31] M. S. Block, D. N. Sheng, O. I. Motrunich, and M. P. A. Fisher, Phys. Rev. Lett. **106**, 157202 (2011).  
[32] C. Gros, Phys. Rev. B **38**, 931(R) (1988); Ann. Phys. (N.Y.) **189**, 53 (1989).  
[33] D. Ceperley, G. V. Chester, and M. H. Kalos, Phys. Rev. B **16**, 3081 (1977).  
[34] S. Bieri, M. Serbyn, T. Senthil, and P. A. Lee, Phys. Rev. B **86**, 224409 (2012).  
[35] D. A. Huse and V. Elser, Phys. Rev. Lett. **60**, 2531 (1988).  
[36] W. LiMing, G. Misguich, P. Sindzingre, and C. Lhuillier, Phys. Rev. B **62**, 6372 (2000).  
[37] L. Capriotti, A. E. Trumper, and S. Sorella, Phys. Rev. Lett. **82**, 3899 (1999).  
[38] S. R. White and A. L. Chernyshev, Phys. Rev. Lett. **99**, 127004 (2007).  
[39] V. Kalmeyer and R. B. Laughlin, Phys. Rev. Lett. **59**, 2095 (1987).



- [40] X.-G. Wen, F. Wilczek, and A. Zee, Phys. Rev. B **39**, 11413 (1989).
- [41] T. Jolicoeur, E. Dagotto, E. Gagliano, and S. Bacci, Phys. Rev. B **42**, 4800 (1990).
- [42] P. Lecheminant, B. Bernu, C. Lhuillier, and L. Pierre, Phys. Rev. B **52**, 6647 (1995).
- [43] A. C. Potter and P. A. Lee, arXiv:1303.6956 (unpublished).
- [44] G. Misguich, C. Lhuillier, B. Bernu, and C. Waldtmann, Phys. Rev. B **60**, 1064 (1999).
- [45] T. Momoi, K. Kubo, and K. Niki, Phys. Rev. Lett. **79**, 2081 (1997).
- [46] L. Messio, C. Lhuillier, and G. Misguich, Phys. Rev. B **83**, 184401 (2011).
- [47] Interestingly, in contrast to the SU(2) case discussed in the present paper, Gutzwiller projected density wave states with three flavors of fermionic spinons clearly outperform Huse-Elser wave functions for SU(3) antiferromagnets on the triangular lattice [34].
- [48] O. I. Motrunich, private communications.
- [49] S.-S. Lee, P. A. Lee, and T. Senthil, Phys. Rev. Lett. **98**, 067006 (2007).